JMST Advances (2019) 1:49–55
https://doi.org/10.1007/s42791-019-0004-2

Online ISSN 2524-7913
Print ISSN 2524-7905

LETTER

Fast Fourier transform solver for damage modeling of composite materials

Yang Chen[1,2] · Dmytro Vasiukov[1,2] · Lionel Gélébart[3] · Chung Hae Park[1,2]

Received: 15 June 2018 / Accepted: 17 February 2019 / Published online: 12 April 2019

Abstract
In the case of highly heterogeneous microstructures, such as textile composites herein, conformal FE meshes are difficult to generate for image-based modeling. As an alternative way regular meshing based on the initial image discretization can be used. However, it requires a large number of elements to reduce undesirable effects due to the voxelized discretization of the phase, such as so-called checkerboard pattern. In this work FAST Fourier transform (FFT) based method has been employed by virtue of its simplicity of meshing and efficiency of parallel computation. One of the major contributions is the extension of the FFT method to nonlinear material modeling based on continuous damage mechanics (CDM). Simple test cases are provided to validate the model. In the last part, the FFT with CDM modeling is applied to a real mesostructure of 3D interlock composite from X-ray computed tomography image.

Keywords Continuous damage mechanics · Fast Fourier transform · Interlock composites

1 Introduction

By virtue of the development of advanced imaging techniques such as 3D Electron Back-Scattered Diffraction (EBSD), X-ray diffraction and X-ray/neutron tomography, image-based modeling is increasingly used to predict the properties of composite materials. Such a modeling strategy has a great advantage of providing the real description of complex 3D microstructure, including irregular geometrical fluctuations and random manufacturing defects, hence making the prediction of material properties more reliable compared with that from an idealized/virtual microstructure. The image-based modeling consists of four main steps: (i) imaging of the considered material; (ii) meshing, i.e., generating a discretize mesh/grid of the microstructure from the digital image; (iii) application of prediction models (elastic, damage, etc.) to the local constitutive materials; (iv) computation using an appropriate solver. Generally, the imaging step involves multidisciplinary technologies and is conducted by specialists, while the material scientists take over the acquired images to complete the subsequent three steps. The meshing step is closely linked to the numerical method to be used, and the most common one is finite element method (FEM) by dint of its versatility. However, meshing for FEM is generally a tedious step especially for the complex microstructure of composites, such as textile composites. In this context, conformal FE meshing with a good quality is a difficult task and has already been the subject of many researches [1–3]. Regular meshing based on the initial image discretization is an alternative way to simplify this processing. However, it requires a large number of elements to reduce undesirable effects due to the structured discretization of the phase interfaces (e.g., see [4, 5] for an illustration).

As an alternative to FEM, fast Fourier transform (FFT) based methods [6–10] become more and more attractive for image-driven modeling of material properties, because they provide great advantages in meshing procedure and parallel computation. The FFT-based methods intrinsically use regular grids to describe the microstructural geometry. Hence, the initial image voxels are directly used as discretized elements without any additional meshing treatment.

Even though the FFT-based methods have been extended to the modeling of nonlinear material behaviors

✉ Chung Hae Park
chung-hae.park@imt-lille-douai.fr

[1] IMT Lille Douai, Institut Mines-Télécom, Douai, France

[2] Université de Lille, Lille, France

[3] DEN-Service de Recherches Métallurgiques Appliquées, CEA, Université Paris-Saclay, Gif-sur-Yvette, France

such as viscoelasticity, plasticity, etc., their application with damage models is not yet very popular. It has been applied to non-local fracture model using a simple criterion on maximum stress [11]. Recently, the FFT-based method was used within a specific algorithm to take into account continuum damage model (CDM) [12]: for each loading step, a linear elastic problem was solved with an FFT-based solver and the resultant stresses were used to evaluate the damage field and update the elastic stiffness fields for the next loading step.

We incorporate a CDM into a generic FFT method to predict the mechanical properties of 3D textile composite material from its micro-architecture, the properties of its constituents and the manufacturing defects such as voids. A massive parallel FFT-based solver (AMITEX) interfaces with CDM through a generic UMAT subroutine (common to ABAQUS and CAST3 M). After a brief description of the proposed model, several numerical test cases are presented to discuss the efficiency of the proposed model. The effect of boundary conditions is investigated using a real 3D interlock composite image by X-ray computed tomography.

2 FFT-based methods

2.1 Numerical algorithm

The local mechanical response of a composite material is obtained by the local equilibrium equation (Eq. 1a), local constitutive law (Eq. 1b) and loading and boundary conditions.

$$\operatorname{div}(\sigma(x)) = 0 \tag{1a}$$

$$\sigma(x) = \mathbb{C}(d(x)) : \varepsilon(x) \tag{1b}$$

where $\sigma(x)$ and $\varepsilon(x)$ are stress and strain tensors, respectively, and $\mathbb{C}(d(x))$ represents the local stiffness matrix which can be degraded by damage state $d(x)$. Considering an auxiliary problem with a homogeneous reference material stiffness $\mathbb{C}_0$, a polarization term is introduced as $\tau(x) = \left(\mathbb{C} - \mathbb{C}_0\right) : \varepsilon(x)$. Then, the solution of the auxiliary problem can be rewritten into the form of Lippmann–Schwinger equation:

$$\varepsilon(x) + (\Gamma_0 * \tau)(x) = E \tag{2}$$

where Γ_0 is the Green operator and E is the prescribed macroscopic strain. In the basic scheme proposed in [6] (Table 1), Eq. 2 is solved with fixed-point algorithm. The variables to be solved in FFT-based methods are strains or stresses, instead of displacements for FEM. With periodic boundary conditions, the stress/strain fields over a regular grid can be transformed into discretized Fourier space. The convolution product with the Green operator (Eq. 2) is converted to a simple multiplication in Fourier space. Such an algorithm (Table 1) is very suitable for parallel computation, because:

Table 1 The basic scheme proposed by [6]

$t=0$	$\varepsilon^0(x) = E$	(T1)
Loop		
$t=k$	$\sigma^k = \sigma\left(\varepsilon^k(x), d_i\right)$	(T2)
	Convergence test	
	$\tau^k(x) = \sigma^k(x) - \mathbb{C}_0 : \varepsilon^k(x)$	(T3)
	FFT: $\tau^k(x) \rightarrow \hat{\tau}^k(\xi)$	(T4)
$t=k+1$	$\hat{\varepsilon}^{k+1}(\xi) = -\left(\hat{\Gamma}_0 \cdot \hat{\tau}^k\right)(\xi)$	(T5)
	Inverse FFT: $\varepsilon^{(k+1)}(\xi)\varepsilon^{(k+1)}(x)$	(T6)

i. (Eqs. T2, T3, T5) are local and can be solved separately for each material point;

ii. The FFT and inverse FFT are not local, but various packages (e.g., parallel FFTW) are available to efficiently complete these two steps in a parallel way.

A code based on this basic scheme (AMITEX [13]) was employed in the present work. This code allows massive parallel simulations on a large number of processors. In addition, it incorporates a procedure accelerating the convergence of the fixed-point algorithm, inspired from the FEM code CAST3M [14], as well as a modified Green operator, as proposed by [15]. As a result, the convergence in AMITEX is faster than the original basic scheme and much less sensitive to the choice of reference material. This FFT algorithm converges efficiently when a progressive damage develops. However, a convergence issue is observed as soon as instable propagation occurs. To address this issue, the FFT algorithm was embedded in an additional loop. If the number of iterations of the FFT algorithm reached a predefined maximum number, the damage variables evaluated during the last iteration were updated and the FFT algorithm (Table 1) was restarted for the same time step. This procedure was also inspired from the FEM code CAST3M.

2.2 Material behavior model

The local constitutive behavior (Eq. T2) obeys the CDM model used for textile composites by [4]. This damage model takes into account the anisotropic elastic and failure properties of the yarns. The homogeneous properties of yarns can be deduced from either analytical models [16, 17], or numerical models at a microscopic length level [18, 19]. As the first attempt, the parameters (listed in Table 2) have been approximately estimated by combining two analytical models [16, 17] as well as by the numerical results in [18]. The damage anisotropy is modeled by three damage variables (d_1, d_2, d_3) corresponding to the three local coordinate

Table 2 Material properties

Yarn	Young's modulus E_{11} (GPa)	44.4
	Young's modulus $E_{22}=E_{33}$ (GPa)	11.64
	In-plane shear modulus G_{12} (GPa)	4.48
	Poisson ratio $v_{12}=v_{13}$	0.26
	Poisson ratio v_{23}	0.33
	Longitudinal strength in tension X_{LT} (MPa)	1500
	Longitudinal strength in compression X_{LC} (MPa)	1000
	Transverse strength in tension X_{TT} (MPa)	60
	Transverse strength in compression X_{TC} (MPa)	150
	Shear strength X_S (MPa)	50
	Fracture energy of yarns in longitudinal direction (kJ)	11
	Fracture energy of yarns in transverse direction (kJ)	0.2
Matrix	Modulus of the matrix E_m (GPa)	3
	Tension/compression strength of matrix X_m (MPa)	80
	Shear strength $X_{m,S}$ (MPa)	40
	Fracture energy of matrix (kJ)	2

axes, i.e., the longitudinal and the two transverse directions, respectively.

This model was implemented in a user subroutine UMAT supported by AMITEX. It should be noted that the damage model incorporates a regularization scheme based on Bazant's crack band model [20], so that the mesh dependency on dissipated fracture energy can be minimized.

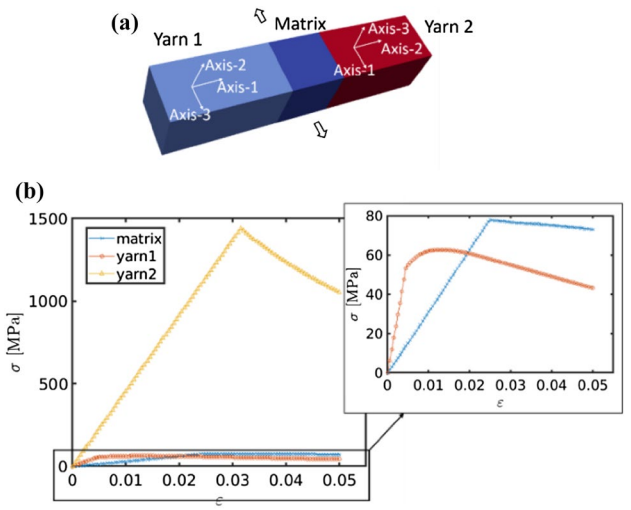

Fig. 1 **a** Unit cell of five voxels: yarn 1 is transverse to the tension, while yarn 2 is parallel to the tension. **b** Stress–strain curves of the three phases simulated by the FFT model

3 Results and discussion

3.1 Test cases

Firstly, to check the implementation of the CDM model, a numerical test was run over a unit cell of five voxels as shown in Fig. 1a. The stress–strain curves in different phases were clearly different (Fig. 1b), showing that the anisotropies were correctly implemented in the model. In this example, the transverse yarn (yarn 1) was damaged before the matrix. The damage evolution in each phase was relatively slow (a moderate decrease rate of the stress). This is strongly linked to the choice of the fracture energies and the characteristic length (80 μm) for damage regularization [20]. It should be noted that the choice used herein was only a first approximation, and more sophisticated homogenization methods (either analytical or numerical) could be adopted to further improve the prediction of the effective properties of yarns.

The second test was performed over a unit cell containing a yarn embedded in matrix. Tensions in longitudinal and transverse directions were applied to the unit cell. The macroscopic stress–strain curves are shown in Fig. 2a. The longitudinal tension produced two sequential changes of slope, corresponding to the damage initiations in the matrix and

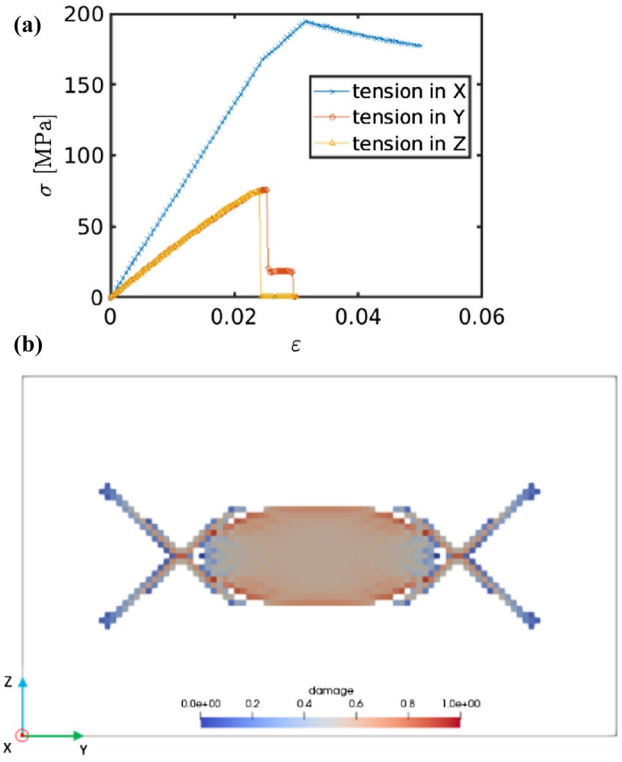

Fig. 2 **a** Macroscopic stress–strain relations of the unit cell with one yarn embedded in matrix under tensions in different directions. **b** Damage field of the unit cell under tension in z-axis (d_2 for the yarn)

in the yarn, respectively. The transverse tensions (in y- and z-axes) led to a quasi-brittle behavior, which was consistent with the fact that once the transverse yarn started to be damaged, the matrix could not provide any more resistance, and the damage would propagate rapidly in the matrix phase. The damage field of the unit cell under tension in Z direction ($\overline{\varepsilon_{zz}} = 2.4\%$) is shown in Fig. 2b. The damage paths in matrix were inclined to the loading direction, suggesting that the matrix was easier to be fractured under shear mode than under tension mode. It should be noted that this property obtained by simulations is related to the damage functions used in the damage model and the chosen material properties (Table 2).

Lastly, we applied the proposed model to a unit cell containing two perpendicular yarns embedded in the matrix (Fig. 3). Tension was applied in the direction along one of the two yarns. The first decrease of stress in the macroscopic curve (Fig. 3a) corresponded to the damage initiation in the transverse yarn, and the final failure was related to the fracture of the longitudinal yarn. This can be confirmed by the damage evolution shown in Fig. 3b. The damage of the longitudinal yarn appeared later after the matrix was considerably fractured, and its path was connected to that of the matrix. The matrix damage paths seemed to be rebounded at the unit cell borders, which was the consequence of the periodic boundary conditions prescribed by the FFT-based method. It is noticeable that different damage modes have been activated in the two yarns: longitudinal damage (d_1) in the longitudinal yarn (green) and transverse damage (d_2) in the transverse yarn (yellow).

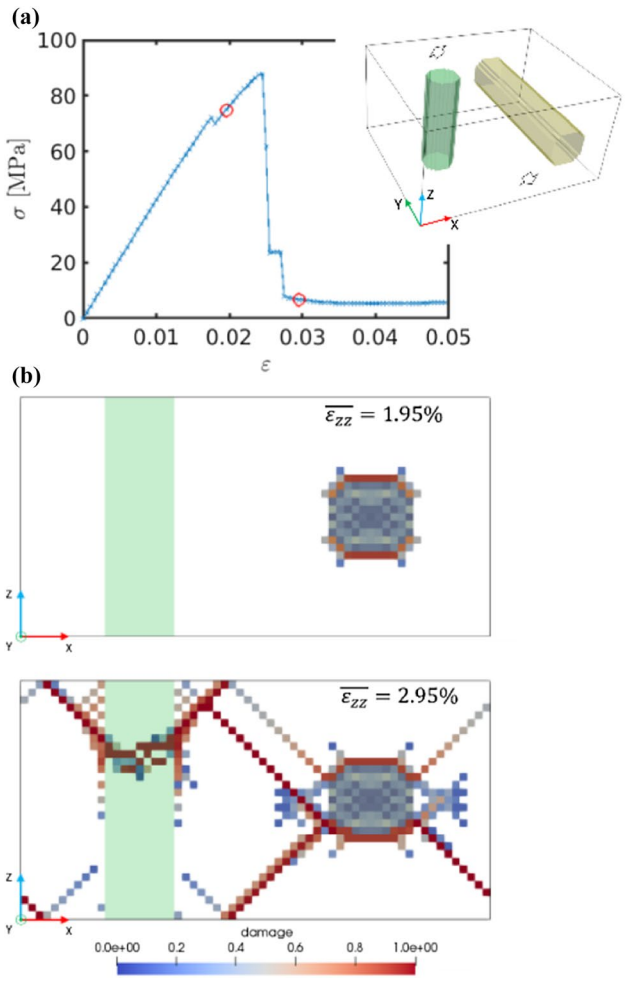

Fig. 3 **a** Macroscopic stress–strain relation of the unit cell with two perpendicular yarns under tension in z-axis. **b** A slice of damage field of the unit cell under two load levels marked by the red circles in **a**. Only the damage values between 0.1 and 1 are shown in the figure

4 Application to 3D interlock composites

4.1 Imaging and unit cell generation

A 3D interlock composite plate was scanned under the X-ray computed tomography of the ISIS4D platform (LML/LaMcube, France). The 3D images were reconstructed and provided a field of view (FOV) of $13.71 \times 3.14 \times 9.99$ mm^3 with a voxel size of 8.8 µm. This FOV contained one pseudo-periodic representative volume element (RVE) of the interlock architecture. For unit cell generation, we used the structure-tensor based method proposed by [21]. Warps, wefts matrix and macrovoids were identified using supervised clustering with the gray-level and local orientation information.

The unit cell contained about 450 million elements ($1407 \times 323 \times 987$ voxels). Even though the FFT-based methods have been proven to provide a great advantage for parallel computation [22], such simulations are very heavy. To save the computational cost, we chose to decrease the unit cell resolution (i.e., number of elements). A unit cell with element size of 185 µm ($15 \times 69 \times 49$ voxels) has been generated (Fig. 4).

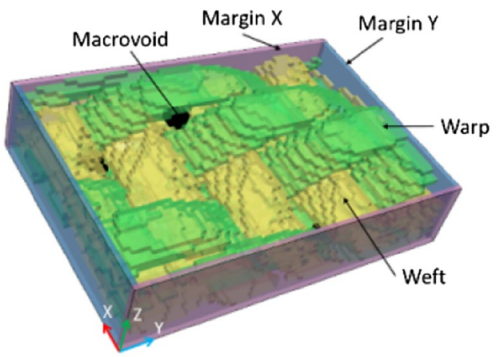

Fig. 4 Reconstructed unit cell of the real mesostructure of the 3D interlock composite with defects (the matrix is hidden)

4.1.1 Edge effect

Periodic boundary conditions (PBC) are intrinsically prescribed by the FFT-based methods. However, a real microstructure is never perfectly periodic. If the local response of the unit cell is of interest, which is more and more demanded for image-based modeling, the edge effect due to the PBC on a non-periodic real microstructure should be considered. To reduce the edge effect, we added marginal layers around the unit cell (see Fig. 4). These marginal layers were assigned with different elastic (non-damageable) properties according to the loading direction: for the loading in x-axis (weft direction), the elastic modulus of margin Y would be set to zero, while that of margin X was greater than zero; vice versa for loading in y-axis (warp direction). The stiffness of the marginal layers (called marginal stiffness hereafter) should be as high as possible because they could act as the role of uniformly transmitting the load between the two corresponding borders.

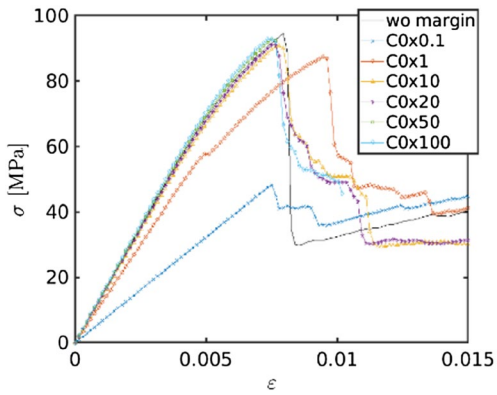

Fig. 5 Macroscopic stress–strain curves of the unit cell: results from the simulations using different marginal stiffness (the stiffness of epoxy matrix was used as a reference C0), compared with that from the simulation without marginal layer

Simulation of such a unit cell (50,715 elements) was parallelized over 12 processors and each iteration took about 0.88 s.

Figure 5 shows the effect of the marginal stiffness on the macroscopic behavior of the composite, compared with the result from the unit cell without marginal layers. The elastic modulus and strength increased with the marginal stiffness and trended to be stable after the marginal stiffness reached 60 GPa (C0x20). The result from the simulation without marginal layer was similar to those with high marginal stiffness. Nevertheless, their local damage fields at the same loading level ($\bar{\varepsilon} = 13.5\%$) were very different, as shown in Fig. 6.

The simulation using no marginal layer led to the prediction of the damage strongly localized at the unit cell borders due to the geometrical discontinuity, whereas those with high marginal stiffness resulted in the prediction of the damage inside the composite. The damage fields obtained from C0x20 and C0x100 were very similar with each other, which again confirmed that the damage prediction became stable and independent on the marginal stiffness if the marginal stiffness became greater than 60 GPa (C0x20). On the other hand, a higher marginal stiffness (> 150 GPa, C0x50) led to a slow convergence rate of the computation once the damage was initiated. Therefore, as a compromise between the prediction accuracy and computation speed, we chose 60 GPa (C0x20) as the elastic modulus of the marginal layers for further simulations.

5 Conclusion

The CDM model has been successfully introduced into the generic FFT-based code. Several test cases showed the damage anisotropy was well considered in the model. The model was then applied to a real mesostructure of a 3D interlock composite to evaluate the effective properties of composites

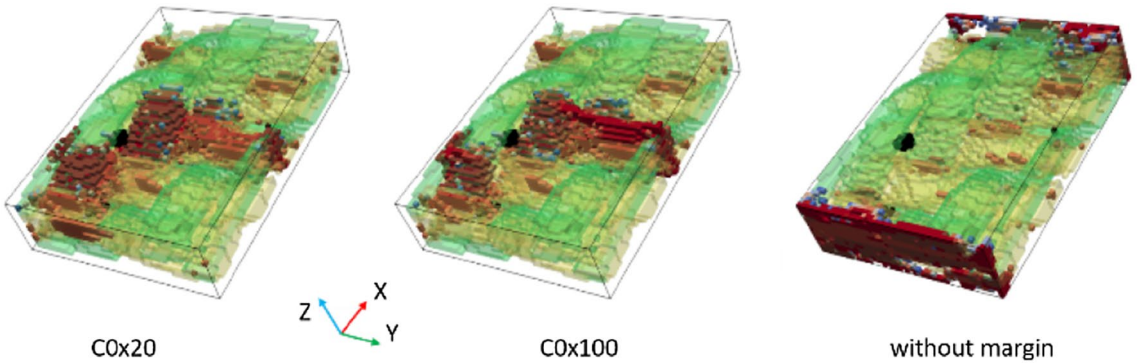

Fig. 6 Damage of the unit cell under tension in warp direction: results from the simulations using three different stiffness of marginal layers. Only the damage values between 0.8 and 1 are shown in the figure

considering the void defects. To reduce the edge effect, elastic marginal layers were added around the unit cell. The effect of the marginal stiffness was investigated, and we proved that the marginal layers were particularly necessary for damage modeling in a real microstructure which was not perfectly periodic. The efficiency of the FFT-based methods for the damage modeling was demonstrated with respect to parallel computation, which cannot be easily achieved by FEM.

Acknowledgements The Nord-Pas-de-Calais Region and the European Community (FEDER funds) partly funds the X-ray tomography equipment ISIS4D platform (LML/LaMcube, France).

References

1. J. Schöberl, An advancing front 2D/3D-mesh generator based on abstract rules. Comput. Vis. Sci. **1**, 41–52 (1997)
2. V.R. Coffman, A.C.E. Reid, S.A. Langer, G. Dogan, OOF3D: an image-based finite element solver for materials science. Math. Comput. Simul. **82**, 2951–2961 (2012)
3. G. Legrain, P. Cartraud, I. Perreard, N. Moes, An X-FEM and level set computational approach for image-based modelling: application to homogenization. Int. J. Numer. Methods Eng. **86**, 915–934 (2011)
4. Y. Liu, I. Straumit, D. Vasiukov, S.V. Lomov, S. Panier, Prediction of linear and non-linear behavior of 3D woven composite using mesoscopic voxel models reconstructed from X-ray microtomography. Compos. Struct. **179**, 568–579 (2017)
5. A. Doitrand, C. Fagiano, F.X. Irisarri, M. Hirsekorn, Comparison between voxel and consistent meso-scale models of woven composites. Compos. A Appl. Sci. Manuf. **73**, 143–154 (2015)
6. H. Moulinec, P. Suquet, A numerical method for computing the overall response of nonlinear composites with complex microstructure. Comput. Methods Appl. Mech. Eng. **157**, 69–94 (1998)
7. S. Brisard, L. Dormieux, FFT-based methods for the mechanics of composites: a general variational framework. Comput. Mater. Sci. **49**, 663–671 (2010)
8. L. Gélébart, R. Mondon-Cancel, Non-linear extension of FFT-based methods accelerated by conjugate gradients to evaluate the mechanical behavior of composite materials. Comput. Mater. Sci. **77**, 430–439 (2013)
9. J. Zeman, T.W.J. de Geus, J. Vondřejc, R.H.J. Peerlings, M.G.D. Geers, A finite element perspective on nonlinear FFT-based micromechanical simulations. Int. J. Numer. Methods Eng. **111**, 903–926 (2017)
10. M. Schneider, D. Merkert, M. Kabel, FFT-based homogenization for microstructures discretized by linear hexahedral elements. Int. J. Numer. Methods Eng. **109**, 1461–1489 (2017)
11. J. Li, S. Meng, X. Tian, F. Song, C. Jiang, A non-local fracture model for composite laminates and numerical simulations by using the FFT method. Compos. B Eng. **43**, 961–971 (2012)
12. B. Wang, G. Fang, S. Liu, M. Fu, J. Liang, Progressive damage analysis of 3D braided composites using FFT-based method. Compos. Struct. **192**, 255–263 (2018)
13. Home AMITEX_FFTP 2.3 documentation http://www.maisondelasimulation.fr/projects/amitex/html/. Accessed 1 Jan 2019
14. Cast3M http://www-cast3m.cea.fr/. Accessed 1 Jan 2019
15. F. Willot, Fourier-based schemes for computing the mechanical response of composites with accurate local fields. C. R. Mec **343**, 232–245 (2015)
16. B. Rosen, Mechanics of composite strengthening, *Fiber composite materials* (ACM, Metals Park, 1964)
17. C. Chamis, Mechanics of composite materials: past, present, and future. J. Compos. Technol. Res. **11**, 3–14 (1989). https://doi.org/10.1520/CTR10143J
18. D. Ashouri Vajari, C. González, J. Llorca, B.N. Legarth, A numerical study of the influence of microvoids in the transverse mechanical response of unidirectional composites. Compos. Sci. Technol. **97**, 46–54 (2014)
19. F. Naya, C. González, C.S. Lopes, S. Van der Veen, F. Pons, Computational micromechanics of the transverse and shear behavior of unidirectional fiber reinforced polymers including environmental effects. Compos. A Appl. Sci. Manuf. **92**, 146–157 (2017)
20. Z.P. Bazant, B.H. Oh, Crack band theory for fracture of concrete. Matériaux Constr. **16**, 155–177 (1983)
21. I. Straumit, S.V. Lomov, M. Wevers, Quantification of the internal structure and automatic generation of voxel models of textile composites from X-ray computed tomography data. Compos. A Appl. Sci. Manuf. **69**, 150–158 (2015)
22. Y. Chen, L. Gélébart, C. Chateau, M. Bornert, C. Sauder, A. King, Analysis of the damage initiation in a SiC/SiC composite tube from a direct comparison between large-scale numerical simulation and synchronoton X-ray micro-tomography. Int. J. Solids Struct. **161**, 111–126 (2019)

Yang Chen obtained BSc in theoretical mechanics, 2008–2013, from Hohai University (China), BSc in theoretical mechanics, 2011–2013, from Université de Lille 1 (France), Masters in computational mechanics, 2013–2014, from Ecole Normale Supérieure de Cachan (France), PhD, 2014–2017, from Université de Paris Est (France)/Navier Laboratory, Post doc, 2017–2018, from IMT Lille Douai (France) and is currently pursuing, 2018–present, Post doc at the University of Oxford (UK). His research fields include computational mechanics, X-ray computed tomography, and image processing for crack detection and quantification.

Dmytro Vasiukov obtained BSc in mechanical engineering, 2002–2006, from National Technical University "Kharkiv Polytechnic Institute" (Ukraine), MSc in mechanical engineering, 2006–2008, from National Technical University, "Kharkiv Polytechnic Institute" (Ukraine), PhD in mechanical engineering, 2010–2013, from Ecole Nationale Supérieure des Mines de Douai (France) and is currently working as an assistant professor, 2013–present, in IMT Lille Douai (France). His research fields include multi-scale material modeling, composite structures, and textile-reinforced materials.

Lionel Gélébart obtained a degree in mechanics, 1994–1999, from Ecole Normale Supérieure de Cachan (France), PhD, 1999–2002, from Ecole Polytechnique/Solid Mechanics Laboratory (France), and is currently a research engineer, 2002–present, at CEA Paris-Saclay University (France)—DEN/DMN/SRM. His research fields include simulation and characterization of the mechanical behavior of heterogeneous materials and since 2013, development of the massively parallel FFT-based code AMITEX_FFTP.

Chung Hae Park obtained BSc in mechanical engineering, 1992–1996, from Seoul National University (Korea), MSc in mechanical engineering, 1996–1998, from Seoul National University (Korea), PhD in mechanical and aerospace engineering, 1998–2003, from Seoul National University (Korea), PhD in mechanical and materials engineering, 2000–2003, from Ecole Nationale Supérieure des Mines de Saint-Etienne (France). He was a senior research engineer at LG Chem (Korea) from 2003 to 2005, a contractual professor at the Université du Havre (France) from 2005 to 2006, an assistant and associate professor at the Université du Havre (France) from 2006 to 2013, obtained a Habilitation à Diriger des Recherche in Mechanics in 2011 from the Université du Havre (France) and is currently, 2013–present, a Full professor at IMT Lille Douai (France). His research fields include manufacturing processes of composite and hybrid structures, numerical methods for simulation and optimization, and mechanics of composite materials.